ECCOMAS Congress 2016
VII European Congress on Computational Methods in Applied Sciences and Engineering
M. Papadrakakis, V. Papadopoulos, G. Stefanou, V. Plevris (eds.)
Crete Island, Greece, 5–10 June 2016

MODELING OF PHASE CHANGES IN MICRO-DOMAIN INDUCED BY AN ULTRASHORT LASER PULSE

Ewa Majchrzak[1], **Lukasz Turchan**[2], **and Jolanta Dziatkiewicz**[2]

[1] Silesian University of Technology
44-100 Gliwice, Konarskiego 18A, Poland
e-mail: ewa.majchrzak@polsl.pl

[2] Silesian University of Technology
44-100 Gliwice, Konarskiego 18A, Poland
lukasz.turchan@polsl.pl, jolanta.dziatkiewicz@polsl.pl

Keywords: microscale heat transfer, two-temperature model, phase transitions, finite difference method.

Abstract. *An axisymmetric micro-domain subjected to the ultrashort laser pulse is considered. To describe the process of heat conduction occurring in the analyzed domain, the two-temperature hyperbolic model together with the isothermal solid-liquid and liquid-vapor phase changes is applied. This model, consisting of four equations describing the electrons and lattice temperatures and also the electrons and lattice heat fluxes, is transformed to the model consisting of only two equations describing the electrons and lattice temperatures. Derived equations together with the appropriate boundary and initial conditions, are solved using the finite difference method supplemented by additional numerical procedures which allow to take into account the phase changes. In the final part of the paper the results of computations are shown and the conclusions are formulated.*

1 INTRODUCTION

Analysis of thermal processes occurring in the micro-domains subjected to an ultrashort laser pulse is of vital importance in microtechnology applications [1]. It should be noted that taking into account the extreme temperature gradients, extremely short duration of the process and the domain dimensions expressed in nanometers, the macroscopic heat conduction equation basing on the Fourier law cannot be applied [2-5]. So, to analyze the process, various alternative mathematical models can be used, for example the two-temperature hyperbolic model [6-10]. At high power of laser the phase transitions can occur this means melting and evaporation. In this paper the axisymmetric two-temperature hyperbolic model together with the isothermal solid–liquid and liquid-vapor phase changes is discussed. This model, presented in the chapter 2, consists of four equations describing the electrons and lattice temperatures and also the electrons and lattice heat fluxes. In chapter 3, using appropriate mathematical transformations, the model consisting of two equations describing only the electrons and lattice temperatures is proposed. Chapter 4 contains the description of numerical algorithm based on the finite difference method, while in the chapter 5 the results of computations are shown. In the final part of the paper the conclusions are formulated.

2 GOVERNING EQUATIONS

Axisymmetric two-temperature model describing the temporal and spatial evolution of the lattice and electrons temperatures in the irradiated metal together with the isothermal solid–liquid and liquid-vapor phase changes is of the form [6-8]

$$C_e(T_e)\frac{\partial T_e(r,z,t)}{\partial t} = -\nabla\cdot\mathbf{q}_e(r,z,t) - G(T_e,T_l)\left[T_e(r,z,t)-T_l(r,z,t)\right] + Q(r,z,t) \tag{1}$$

$$C_l\frac{\partial T_l(r,z,t)}{\partial t} = -\nabla\cdot\mathbf{q}_l(r,z,t) + G(T_e,T_l)\left[T_e(r,z,t)-T_l(r,z,t)\right] + Q_m(r,z,t) + Q_{ev}(r,z,t) \tag{2}$$

where $T_e\,(r, z, t)$, $T_l\,(r, z, t)$, $\mathbf{q}_e\,(r, z, t)$, $\mathbf{q}_l\,(r, z, t)$ are the temperatures and heat fluxes of the electrons and lattice, respectively, $C_e\,(T_e)$, C_l are the volumetric specific heats, $G(T_e, T_l)$ is the electron-phonon coupling factor which characterizes the energy exchange between electrons and phonons, $Q(r, z, t)$ is the source function associated with the irradiation, while $Q_m(r, z, t)$ and $Q_{ev}(r, z, t)$ are the source functions associated with the melting and evaporation, respectively.

In a place of classical Fourier law the following formulas are introduced

$$\mathbf{q}_e(r,z,t) + \tau_e\frac{\partial\mathbf{q}_e(r,z,t)}{\partial t} = -\lambda_e(T_e,T_l)\nabla T_e(r,z,t) \tag{3}$$

$$\mathbf{q}_l(r,z,t) + \tau_l\frac{\partial\mathbf{q}_l(r,z,t)}{\partial t} = -\lambda_l\nabla T_l(r,z,t) \tag{4}$$

where $\lambda_e\,(T_e\,,\,T_l)$, λ_l are the thermal conductivities of the electrons and lattice, respectively, τ_e is the relaxation time of free electrons in metals (the mean time for electrons to change their states), τ_l is the relaxation time in phonon collisions and $\nabla(\cdot)$ denotes the gradient.

The laser irradiation is described by a source term introduced in equation (1) [11, 12]

$$Q(r,z,t) = \sqrt{\frac{4\ln 2}{\pi}}\left(1-R\right)\frac{I_0}{\delta t_p}\exp\left[-\frac{r^2}{r_D^2}-\frac{z}{\delta}-4\ln 2\frac{\left(t-2t_p\right)^2}{t_p^2}\right] \tag{5}$$

where I_0 is the laser intensity, t_p is the characteristic time of laser pulse, δ is the optical penetration depth, R is the reflectivity of the irradiated surface and r_D is the laser beam radius.

The internal heat sources resulting from the phase changes (melting and evaporation) take a form [13-15]

$$\begin{aligned} Q_m(r,z,t) &= -L_m \frac{\partial S_m(r,z,t)}{\partial t} \\ Q_{ev}(r,z,t) &= -L_{ev} \frac{\partial S_{ev}(r,z,t)}{\partial t} \end{aligned} \tag{6}$$

where L_m is the volumetric heat of fusion, L_{ev} is the volumetric heat of evaporation, S_m and S_{ev} are the volumetric molten and gaseous state fractions in the surroundings of the point considered. Both S_m and S_{ev} are equal to zero at the beginning of heating process and increase from 0 to 1 when the local temperature achieves the melting T_m and boiling T_{ev} temperatures, respectively.

The above presented mathematical model is supplemented by the boundary conditions (no-flux conditions), it means

$$(r,\ z) \in \Gamma: \quad \begin{aligned} q_{be}(r,\ z,\ t) &= -\lambda_e(T_e,T_l)\ \mathbf{n} \cdot \nabla T_e(r,z,t) = 0 \\ q_{bl}(r,\ z,\ t) &= -\lambda_l\ \mathbf{n} \cdot \nabla T_l(r,z,t) = 0 \end{aligned} \tag{7}$$

where **n** is the outward unit normal vector.

The initial temperature distribution is also known

$$t = 0: \qquad T_e(r,\ z,\ t) = T_l(r,\ z,\ t) = T_0 \tag{8}$$

where T_0 is constant.

For high laser intensity the following dependencies are used [6, 8, 16]

$$C_e(T_e) = \begin{cases} A T_e, & T_e < T_F / \pi^2 \\ A T_F / \pi^2 + \dfrac{N k_B - A T_F / \pi^2}{2 T_F / \pi^2}\left(T_e - T_F / \pi^2\right), & T_F / \pi^2 \le T_e < 3 T_F / \pi^2 \\ N k_B + \dfrac{N k_B / 2}{T_F - 3 T_F / \pi^2}\left(T_e - 3 T_F / \pi^2\right), & 3 T_F / \pi^2 \le T_e < T_F \\ 3 N k_B / 2, & T_e \ge T_F \end{cases} \tag{9}$$

and

$$\lambda_e(T_e,T_l) = \chi \frac{\left[\left(T_e / T_F\right)^2 + 0.16\right]^{5/4} \left[\left(T_e / T_F\right)^2 + 0.44\right]\left(T_e / T_F\right)}{\left[\left(T_e / T_F\right)^2 + 0.092\right]^{1/2} \left[\left(T_e / T_F\right)^2 + \eta\left(T_l / T_F\right)\right]} \tag{10}$$

while

$$G(T_e,T_l) = G_{rt}\left[\frac{A_e}{B_l}\left(T_e + T_l\right) + 1\right] \tag{11}$$

where T_F is the Fermi temperature, N is the density of electrons, k_B is the Boltzmann constant, $A = \pi^2 N k_B / (2\ T_F)$, χ, η, A_e, B_l are the constants and G_{rt} is the coupling factor at room temperature. Other parameters: λ_l, C_l, τ_e, τ_l are assumed to be constant.

3 MATHEMATICAL MANIPULATIONS

In this chapter, another form of the two-temperature model will be presented. Introducing (3) into (1) and (4) into (2), respectively, one has

$$C_e(T_e)\frac{\partial T_e(r,z,t)}{\partial t}=\nabla\cdot\left[\tau_e\frac{\partial \mathbf{q}_e(r,z,t)}{\partial t}+\lambda_e(T_e,T_l)\,\nabla T_e(r,z,t)\right]- \\ G(T_e,T_l)\left[T_e(r,z,t)-T_l(r,z,t)\right]+Q(r,z,t) \tag{12}$$

and

$$C_l\frac{\partial T_l(r,z,t)}{\partial t}=\nabla\cdot\left[\tau_l\frac{\partial \mathbf{q}_l(r,z,t)}{\partial t}+\lambda_l\,\nabla T_l(r,z,t)\right]+G(T_e,T_l)\left[T_e(r,z,t)-T_l(r,z,t)\right]+ \\ Q_m(r,z,t)+Q_{ev}(r,z,t) \tag{13}$$

Assuming that τ_e and τ_l are the constant values, the equations (12), (13) can be written in the form

$$C_e(T_e)\frac{\partial T_e(r,z,t)}{\partial t}=\tau_e\frac{\partial}{\partial t}\left[\nabla\cdot\mathbf{q}_e(r,z,t)\right]+\nabla\left[\lambda_e(T_e,T_l)\,\nabla T_e(r,z,t)\right]- \\ G(T_e,T_l)\left[T_e(r,z,t)-T_l(r,z,t)\right]+Q(r,z,t) \tag{14}$$

and

$$C_l\frac{\partial T_l(r,z,t)}{\partial t}=\tau_l\frac{\partial}{\partial t}\left[\nabla\cdot\mathbf{q}_l(r,z,t)\right]+\nabla\left[\lambda_l\,\nabla T_l(r,z,t)\right]+ \\ G(T_e,T_l)\left[T_e(r,z,t)-T_l(r,z,t)\right]+Q_m(r,z,t)+Q_{ev}(r,z,t) \tag{15}$$

From equations (1), (2) results that

$$-\nabla\cdot\mathbf{q}_e(r,z,t)=C_e(T_e)\frac{\partial T_e(r,z,t)}{\partial t}+G(T_e,T_l)\left[T_e(r,z,t)-T_l(r,z,t)\right]-Q(r,z,t) \tag{16}$$

and

$$-\nabla\cdot\mathbf{q}_l(r,z,t)=C_l\frac{\partial T_l(r,z,t)}{\partial t}-G(T_e,T_l)\left[T_e(r,z,t)-T_l(r,z,t)\right]- \\ Q_m(r,z,t)-Q_{ev}(r,z,t) \tag{17}$$

Introducing (16) into (14) and (17) into (15), respectively, the equations (14), (15) have a form

$$C_e(T_e)\frac{\partial T_e(r,z,t)}{\partial t}+\tau_e\frac{\partial C_e(T_e)}{\partial t}\frac{\partial T_e(r,z,t)}{\partial t}+\tau_e C_e(T_e)\frac{\partial^2 T_e(r,z,t)}{\partial t^2}= \\ \nabla\left[\lambda_e(T_e,T_l)\,\nabla T_e(r,z,t)\right]-\left[G(T_e,T_l)+\tau_e\frac{\partial G(T_e,T_l)}{\partial t}\right]\left[T_e(r,z,t)-T_l(r,z,t)\right]- \\ \tau_e G(T_e,T_l)\left[\frac{\partial T_e(r,z,t)}{\partial t}-\frac{\partial T_l(r,z,t)}{\partial t}\right]+Q(r,z,t)+\tau_e\frac{\partial Q(r,z,t)}{\partial t} \tag{18}$$

and

$$
\begin{gathered}
C_l \frac{\partial T_l(r,z,t)}{\partial t} + \tau_l C_l \frac{\partial^2 T_l(r,z,t)}{\partial t^2} = \nabla\left[\lambda_l \nabla T_l(r,z,t)\right] + \\
\left[G(T_e,T_l) + \tau_l \frac{\partial G(T_e,T_l)}{\partial t}\right]\left[T_e(r,z,t) - T_l(r,z,t)\right] + \tau_l G(T_e,T_l)\left[\frac{\partial T_e(r,z,t)}{\partial t} - \frac{\partial T_l(r,z,t)}{\partial t}\right] + \\
Q_m(r,z,t) + \tau_l \frac{\partial Q_m(r,z,t)}{\partial t} + Q_{ev}(r,z,t) + \tau_l \frac{\partial Q_{ev}(r,z,t)}{\partial t}
\end{gathered} \tag{19}
$$

Because

$$
\begin{gathered}
\frac{\partial C_e(T_e)}{\partial t} = \frac{\mathrm{d} C_e(T_e)}{\mathrm{d} T_e} \frac{\partial T_e}{\partial t} \\
\frac{\partial G(T_e,T_l)}{\partial t} = \frac{\partial G(T_e,T_l)}{\partial T_e} \frac{\partial T_e}{\partial t} + \frac{\partial G(T_e,T_l)}{\partial T_l} \frac{\partial T_l}{\partial t}
\end{gathered} \tag{20}
$$

therefore

$$
\begin{gathered}
C_e(T_e)\left[\frac{\partial T_e(r,z,t)}{\partial t} + \tau_e \frac{\partial^2 T_e(r,z,t)}{\partial t^2}\right] + \tau_e G(T_e,T_l) \frac{\partial T_e(r,z,t)}{\partial t} = \\
\nabla\left[\lambda_e(T_e,T_l)\,\nabla T_e(r,z,t)\right] - \tau_e \frac{\mathrm{d} C_e(T_e)}{\mathrm{d} T_e}\left[\frac{\partial T_e(r,z,t)}{\partial t}\right]^2 - \\
\left\{G(T_e,T_l) + \tau_e\left[\frac{\partial G(T_e,T_l)}{\partial T_e}\frac{\partial T_e(r,z,t)}{\partial t} + \frac{\partial G(T_e,T_l)}{\partial T_l}\frac{\partial T_l(r,z,t)}{\partial t}\right]\right\}\left[T_e(r,z,t) - T_l(r,z,t)\right] + \\
\tau_e G(T_e,T_l) \frac{\partial T_l(r,z,t)}{\partial t} + Q(r,z,t) + \tau_e \frac{\partial Q(r,z,t)}{\partial t}
\end{gathered} \tag{21}
$$

and

$$
\begin{gathered}
C_l\left[\frac{\partial T_l(r,z,t)}{\partial t} + \tau_l \frac{\partial^2 T_l(r,z,t)}{\partial t^2}\right] + \tau_l G(T_e,T_l) \frac{\partial T_l(r,z,t)}{\partial t} = \nabla\left[\lambda_l \nabla T_l(r,z,t)\right] + \\
\left\{G(T_e,T_l) + \tau_l\left[\frac{\partial G(T_e,T_l)}{\partial T_e}\frac{\partial T_e(r,z,t)}{\partial t} + \frac{\partial G(T_e,T_l)}{\partial T_l}\frac{\partial T_l(r,z,t)}{\partial t}\right]\right\}\left[T_e(r,z,t) - T_l(r,z,t)\right] + \\
\tau_l G(T_e,T_l) \frac{\partial T_e(r,z,t)}{\partial t} + Q_m(r,z,t) + \tau_l \frac{\partial Q_m(r,z,t)}{\partial t} + Q_{ev}(r,z,t) + \tau_l \frac{\partial Q_{ev}(r,z,t)}{\partial t}
\end{gathered} \tag{22}
$$

Finally

$$
\begin{gathered}
\left[C_e(T_e)+\tau_e G(T_e,T_l)\right]\frac{\partial T_e(r,z,t)}{\partial t}+\tau_e C_e(T_e)\frac{\partial^2 T_e(r,z,t)}{\partial t^2}= \\
\nabla\left[\lambda_e(T_e,T_l)\,\nabla T_e(r,z,t)\right]-\tau_e\frac{\mathrm{d}C_e(T_e)}{\mathrm{d}T_e}\left[\frac{\partial T_e(r,z,t)}{\partial t}\right]^2- \\
\left\{G(T_e,T_l)+\tau_e\left[\frac{\partial G(T_e,T_l)}{\partial T_e}\frac{\partial T_e(r,z,t)}{\partial t}+\frac{\partial G(T_e,T_l)}{\partial T_l}\frac{\partial T_l(r,z,t)}{\partial t}\right]\right\}\left[T_e(r,z,t)-T_l(r,z,t)\right]+ \\
\tau_e G(T_e,T_l)\frac{\partial T_l(r,z,t)}{\partial t}+Q(r,z,t)+\tau_e\frac{\partial Q(r,z,t)}{\partial t}
\end{gathered}
\tag{23}
$$

and

$$
\begin{gathered}
C_l\left[\frac{\partial T_l(r,z,t)}{\partial t}+\tau_l\frac{\partial^2 T_l(r,z,t)}{\partial t^2}\right]+\tau_l G(T_e,T_l)\frac{\partial T_l(r,z,t)}{\partial t}=\nabla\left[\lambda_l\,\nabla T_l(r,z,t)\right]+ \\
\left\{G(T_e,T_l)+\tau_l\left[\frac{\partial G(T_e,T_l)}{\partial T_e}\frac{\partial T_e(r,z,t)}{\partial t}+\frac{\partial G(T_e,T_l)}{\partial T_l}\frac{\partial T_l(r,z,t)}{\partial t}\right]\right\}\left[T_e(r,z,t)-T_l(r,z,t)\right]+ \\
\tau_l G(T_e,T_l)\frac{\partial T_e(r,z,t)}{\partial t}+Q_m(r,z,t)+\tau_l\frac{\partial Q_m(r,z,t)}{\partial t}+Q_{ev}(r,z,t)+\tau_l\frac{\partial Q_{ev}(r,z,t)}{\partial t}
\end{gathered}
\tag{24}
$$

Summarizing, the equations (23) and (24) supplemented by boundary conditions (7) and initial condition (8) create an equivalent two-temperature model described in the chapter 2. It should be noted that in this model the second time derivatives appear and therefore the additional initial condition should be introduced

$$
t=0:\quad \left.\frac{\partial T(r,z,t)}{\partial t}\right|_{t=0}=0
\tag{25}
$$

The phase transitions are modeled using the authorial version of the algorithm called ‘a temperature recovery method’ [17]. When the local temperature at the node (i, j) achieves the value of melting point T_m then the source function $Q_m(r_i, z_j, t)$ starts, at the same time, because the melting process proceeds at the constant temperature the derivatives of lattice temperature with respect to time (equation (24)) are equal to 0. So, one has (c.f. equation (24))

$$
\begin{gathered}
0=\nabla\left[\lambda_l\,\nabla T_l(r,z,t)\right]+\left[G(T_e,T_l)+\tau_l\frac{\partial G(T_e,T_l)}{\partial T_e}\frac{\partial T_e(r,z,t)}{\partial t}\right]\left[T_e(r,z,t)-T_m\right]+ \\
\tau_l G(T_e,T_l)\frac{\partial T_e(r,z,t)}{\partial t}-L_m\frac{\partial S_m(r,z,t)}{\partial t}-\tau_l L_m\frac{\partial^2 S_m(r,z,t)}{\partial t^2}
\end{gathered}
\tag{26}
$$

it means

$$
\begin{gathered}
L_m\frac{\partial S_m(r,z,t)}{\partial t}+\tau_l L_m\frac{\partial^2 S_m(r,z,t)}{\partial t^2}=\nabla\left[\lambda_l\,\nabla T_l(r,z,t)\right]+ \\
\left[G(T_e,T_l)+\tau_l\frac{\partial G(T_e,T_l)}{\partial T_e}\frac{\partial T_e(r,z,t)}{\partial t}\right]\left[T_e(r,z,t)-T_m\right]+\tau_l G(T_e,T_l)\frac{\partial T_e(r,z,t)}{\partial t}
\end{gathered}
\tag{27}
$$

The similar equation describes the evaporation process

$$L_{ev}\frac{\partial S_{ev}(r,z,t)}{\partial t}+\tau_l\, L_{ev}\frac{\partial^2 S_{ev}(r,z,t)}{\partial t^2}=\nabla\left[\lambda_l\,\nabla T_l(r,z,\,t)\right]+$$
$$\left[G(T_e,T_l)+\tau_l\frac{\partial G(T_e,T_l)}{\partial T_e}\frac{\partial T_e(r,z,t)}{\partial t}\right]\left[T_e(r,z,\,t)-T_{ev}\right]+\tau_l\, G(T_e,T_l)\frac{\partial T_e\,(r,z,\,t)}{\partial t} \tag{28}$$

4 METHOD OF SOLUTION

To solve the problem formulated in the chapter 3, the finite difference method is used [18, 19]. The geometrical mesh with dimensions $n\times n$ is introduced and the temperatures for time $t^f = f\ \Delta t$ ($f \geq 2$, Δt is the constant time step) at the node (i, j) are denoted as $T_{e\,i,j}^f = T_e(r_j, z_i, t^f)$ and $T_{l\,i,j}^f = T_l(r_j, z_i, t^f)$, respectively.

The following approximation of equation (23) is proposed

$$\left(C_{ei,j}^{f-1}+\tau_e G_{i,j}^{f-1}\right)\frac{T_{ei,j}^{f}-T_{ei,j}^{f-1}}{\Delta t}+\tau_e\, C_{ei,j}^{f-1}\frac{T_{ei,j}^{f}-2T_{ei,j}^{f-1}+T_{ei,j}^{f-2}}{(\,\Delta t)^2}=$$
$$\nabla\left(\lambda_e\,\nabla T_e\right)_{i,j}^{f-1}-\tau_e\left(\frac{\mathrm{d}\,C_e}{\mathrm{d}\,T_e}\right)_{i,j}^{f-1}\frac{\left(T_{ei,j}^{f-1}-T_{ei,j}^{f-2}\right)^2}{(\,\Delta t)^2}-$$
$$\left\{G_{i,j}^{f-1}+\tau_e\left[\left(\frac{\partial G}{\partial T_e}\right)_{i,j}^{f-1}\frac{T_{ei,j}^{f-1}-T_{ei,j}^{f-2}}{\Delta t}+\left(\frac{\partial G}{\partial T_l}\right)_{i,j}^{f-1}\frac{T_{li,j}^{f-1}-T_{li,j}^{f-2}}{\Delta t}\right]\right\}\left(T_{ei,j}^{f-1}-T_{li,j}^{f-1}\right)+ \tag{29}$$
$$\tau_e\left[\left(\frac{\partial G}{\partial T_e}\right)_{i,j}^{f-1}\frac{T_{ei,j}^{f-1}-T_{ei,j}^{f-2}}{\Delta t}+\left(\frac{\partial G}{\partial T_l}\right)_{i,j}^{f-1}\frac{T_{li,j}^{f-1}-T_{li,j}^{f-2}}{\Delta t}\right]\left(T_{ei,j}^{f-1}-T_{li,j}^{f-1}\right)+$$
$$\tau_e G_{i,j}^{f-1}\frac{T_{li,j}^{f-1}-T_{li,j}^{f-2}}{\Delta t}+Q_{i,j}^{f-1}+\tau_e\left(\frac{\partial\, Q}{\partial\, t}\right)_{i,j}^{f-1}$$

where

$$\nabla\left(\lambda_e\nabla T_e\right)_{i,j}^{f-1}=\Phi_1\frac{T_{ei,j-1}^{f-1}-T_{ei,j}^{f-1}}{R_{i,j1}^{f-1}}+\Phi_2\frac{T_{ei,j+1}^{f-1}-T_{ei,j}^{f-1}}{R_{i,j2}^{f-1}}+$$
$$\Phi_3\frac{T_{ei-1,j}^{f-1}-T_{ei,j}^{f-1}}{R_{i,j3}^{f-1}}+\Phi_4\frac{T_{ei+1,j}^{f-1}-T_{ei,j}^{f-1}}{R_{i,j4}^{f-1}} \tag{30}$$

while

$$R_{i,j1}^{f-1}=\frac{h}{2}\left(\frac{1}{\lambda_{ei,j}^{f-1}}+\frac{1}{\lambda_{ei,j-1}^{f-1}}\right),\quad R_{i,j2}^{f-1}=\frac{h}{2}\left(\frac{1}{\lambda_{ei,j}^{f-1}}+\frac{1}{\lambda_{ei,j+1}^{f-1}}\right)$$
$$R_{i,j3}^{f-1}=\frac{h}{2}\left(\frac{1}{\lambda_{ei,j}^{f-1}}+\frac{1}{\lambda_{ei-1,j}^{f-1}}\right),\quad R_{i,j4}^{f-1}=\frac{h}{2}\left(\frac{1}{\lambda_{ei,j}^{f-1}}+\frac{1}{\lambda_{ei+1,j}^{f-1}}\right) \tag{31}$$

are the thermal resistances between adjacent nodes [18, 19] and

$$\Phi_1 = \left(r_{i,j} - 0.5h\right)/\left(h\,r_{i,j}\right), \quad \Phi_2 = \left(r_{i,j} + 0.5h\right)/\left(h\,r_{i,j}\right), \quad \Phi_3 = \Phi_4 = 1/h \tag{32}$$

are the shape functions of differential mesh for the axially-symmetrical task.
After mathematical manipulations one has

$$\begin{gathered}
T_{ei,j}^{f} = \frac{(\Delta t)^2 \nabla\left(\lambda_e \nabla T_e\right)_{i,j}^{f-1}}{\Delta t\left(C_{ei,j}^{f-1} + \tau_e G_{i,j}^{f-1}\right) + \tau_e C_{ei,j}^{f-1}} + \frac{\Delta t\left(C_{ei,j}^{f-1} + \tau_e G_{i,j}^{f-1}\right) + 2\tau_e C_{ei,j}^{f-1}}{\Delta t\left(C_{ei,j}^{f-1} + \tau_e G_{i,j}^{f-1}\right) + \tau_e C_{ei,j}^{f-1}} T_{ei,j}^{f-1} - \\
\frac{\tau_e C_{ei,j}^{f-1} T_{ei,j}^{f-2}}{\Delta t\left(C_{ei,j}^{f-1} + \tau_e G_{i,j}^{f-1}\right) + \tau_e C_{ei,j}^{f-1}} - \frac{\tau_e \left(T_{ei,j}^{f-1} - T_{ei,j}^{f-2}\right)^2}{\Delta t\left(C_{ei,j}^{f-1} + \tau_e G_{i,j}^{f-1}\right) + \tau_e C_{ei,j}^{f-1}} \left(\frac{\mathrm{d} C_e}{\mathrm{d} T_e}\right)_{i,j}^{f-1} - \\
\frac{(\Delta t)^2 \left(T_{ei,j}^{f-1} - T_{li,j}^{f-1}\right)}{\Delta t\left(C_{ei,j}^{f-1} + \tau_e G_{i,j}^{f-1}\right) + \tau_e C_{ei,j}^{f-1}} \left\{ G_{i,j}^{f-1} + \tau_e \left[\left(\frac{\partial G}{\partial T_e}\right)_{i,j}^{f-1} \frac{T_{ei,j}^{f-1} - T_{ei,j}^{f-2}}{\Delta t} + \left(\frac{\partial G}{\partial T_l}\right)_{i,j}^{f-1} \frac{T_{li,j}^{f-1} - T_{li,j}^{f-2}}{\Delta t} \right] \right\} + \\
\frac{\tau_e G_{i,j}^{f-1} \Delta t \left(T_{li,j}^{f-1} - T_{li,j}^{f-2}\right)}{\Delta t\left(C_{ei,j}^{f-1} + \tau_e G_{i,j}^{f-1}\right) + \tau_e C_{ei,j}^{f-1}} + \frac{(\Delta t)^2}{\Delta t\left(C_{ei,j}^{f-1} + \tau_e G_{i,j}^{f-1}\right) + \tau_e C_{ei,j}^{f-1}} \left[Q_{i,j}^{f-1} + \tau_e \left(\frac{\partial Q}{\partial t}\right)_{i,j}^{f-1} \right]
\end{gathered} \tag{33}$$

In a similar way the equation (24) can be approximated and for the temperatures below the melting point one obtains

$$\begin{gathered}
T_{li,j}^{f} = \frac{(\Delta t)^2 \nabla\left(\lambda_l \nabla T_l\right)_{i,j}^{f-1}}{\Delta t\left(C_l + \tau_l G_{i,j}^{f-1}\right) + \tau_l C_l} + \frac{\Delta t\left(C_l + \tau_l G_{i,j}^{f-1}\right) + 2\tau_l C_l}{\Delta t\left(C_l + \tau_l G_{i,j}^{f-1}\right) + \tau_l C_l} T_{li,j}^{f-1} - \\
\frac{\tau_l C_l}{\Delta t\left(C_l + \tau_l G_{i,j}^{f-1}\right) + \tau_l C_l} T_{li,j}^{f-2} + \frac{\tau_l G_{i,j}^{f-1} \Delta t}{\Delta t\left(C_l + \tau_l G_{i,j}^{f-1}\right) + \tau_l C_l} \left(T_{ei,j}^{f-1} - T_{ei,j}^{f-2}\right) + \\
\frac{(\Delta t)^2 \left(T_{ei,j}^{f-1} - T_{li,j}^{f-1}\right)}{\Delta t\left(C_l + \tau_l G_{i,j}^{f-1}\right) + \tau_l C_l} \left\{ G_{i,j}^{f-1} + \tau_l \left[\left(\frac{\partial G}{\partial T_e}\right)_{i,j}^{f-1} \frac{T_{ei,j}^{f-1} - T_{ei,j}^{f-2}}{\Delta t} + \left(\frac{\partial G}{\partial T_l}\right)_{i,j}^{f-1} \frac{T_{li,j}^{f-1} - T_{li,j}^{f-2}}{\Delta t} \right] \right\}
\end{gathered} \tag{34}$$

In turn, the finite difference approximation of equation (27) is of the form

$$\begin{gathered}
L_m \frac{S_{mi,j}^{f} - S_{mi,j}^{f-1}}{\Delta t} + \tau_l L_m \frac{S_{mi,j}^{f} - 2S_{mi,j}^{f-1} + S_{mi,j}^{f-2}}{(\Delta t)^2} = \nabla\left[\lambda_l \nabla T_l(r, z, t)\right]_{i,j}^{f-1} + \\
\left[G_{i,j}^{f-1} + \tau_l \left(\frac{\partial G}{\partial T_e}\right)_{i,j}^{f-1} \frac{T_{ei,j}^{f-1} - T_{ei,j}^{f-2}}{\Delta t} \right] \left(T_{ei,j}^{f-1} - T_m\right) + \tau_l G_{i,j}^{f-1} \frac{T_{ei,j}^{f-1} - T_{ei,j}^{f-2}}{\Delta t}
\end{gathered} \tag{35}$$

and next

$$\begin{gathered}
S_{mi,j}^{f} = \frac{\Delta t + 2\tau_l}{\Delta t + \tau_l} S_{mi,j}^{f-1} - \frac{\tau_l}{\Delta t + \tau_l} S_{mi,j}^{f-2} + \frac{(\Delta t)^2}{L_m(\Delta t + \tau_l)} \nabla\left[\lambda_l \nabla T_l(r, z, t)\right]_{i,j}^{f-1} + \\
\frac{(\Delta t)^2}{L_m(\Delta t + \tau_l)} \left[G_{i,j}^{f-1} + \tau_l \left(\frac{\partial G}{\partial T_e}\right)_{i,j}^{f-1} \frac{T_{ei,j}^{f-1} - T_{ei,j}^{f-2}}{\Delta t} \right] \left(T_{ei,j}^{f-1} - T_m\right) + \frac{\tau_l \Delta t G_{i,j}^{f-1}}{L_m(\Delta t + \tau_l)} \left(T_{ei,j}^{f-1} - T_{ei,j}^{f-2}\right)
\end{gathered} \tag{36}$$

In a similar way one obtains (c.f. equation (28))

$$S_{ev\,i,j}^{f} = \frac{\Delta t + 2\tau_l}{\Delta t + \tau_l} S_{ev\,i,j}^{f-1} - \frac{\tau_l}{\Delta t + \tau_l} S_{ev\,i,j}^{f-2} + \frac{(\Delta t)^2}{L_{ev}(\Delta t + \tau_l)} \nabla\left[\lambda_l \nabla T_l(r,z,t)\right]_{i,j}^{f-1} +$$
$$\frac{(\Delta t)^2}{L_{ev}(\Delta t + \tau_l)} \left[G_{i,j}^{f-1} + \tau_l \left(\frac{\partial G}{\partial T_e}\right)_{i,j}^{f-1} \frac{T_{ei,j}^{f-1} - T_{ei,j}^{f-2}}{\Delta t} \right] \left(T_{ei,j}^{f-1} - T_{ev}\right) + \frac{\tau_l \, \Delta t G_{i,j}^{f-1}}{L_{ev}(\Delta t + \tau_l)} \left(T_{ei,j}^{f-1} - T_{ei,j}^{f-2}\right) \tag{37}$$

5 RESULTS OF COMPUTATIONS

Numerical simulation of a thermal process taking place in the cylindrical domain with dimensions $Z = 100\cdot10^{-9}$ [m] and $R = 100\cdot10^{-9}$ [m] subjected to the short-pulse laser heating has been done. The initial temperature is equal to $T_p = 300$ K. Thermophysical parameters of material are equal to (gold): thermal conductivity of lattice $\lambda_l = 315$ W/(mK), volumetric specific heat of lattice $C_l = 2.5$ MJ/(m^3 K), electrons relaxation time $\tau_e = 0.04$ ps, phonons relaxation time $\tau_l = 0.8$ ps [20], reflectivity $R = 0.93$, optical penetration depth $\delta = 15.3$ nm. The Fermi temperature is equal to $T_F = 64\ 200$ K and the density of electrons is equal to $N = 5.9\cdot10^{28}$ 1/m (c.f. equation (9)) [6]. The constants in equations (10), (11) are the following: $\chi = 353$ W/(mK), $\eta = 0.16$, $A_e = 1.2\cdot10^7$ 1/(K^2 s), $B_l = 1.23\cdot10^{11}$ 1/(Ks) and $G_{rt} = 2.2\cdot10^{16}$ W/(m^{3}K) [6]. The melting point is equal to $T_m = 1336$ K, the boiling point: $T_e = 3127$ K, the volumetric heat of fusion: $L_m = 1.23\cdot10^3$ MJ/m^3 and the volumetric heat of evaporation: $L_{ev} = 3.277\cdot10^4$ MJ/m^3.

The laser beam radius is equal to $r_D = R/8$. The calculations were performed for five values of the laser intensity: $I_0 = 2\cdot10^5$ J/m^2, $I_0 = 4\cdot10^5$ J/m^2, $I_0 = 6\cdot10^5$ J/m^2 , $I_0 = 8\cdot10^5$ J/m^2 and $I_0 = 10^6$ J/m^2 under the assumption that the characteristic time of laser pulse is equal to $t_p = 100$ ps (c.f. formula (5)). The problem is solved using the finite difference method. Number of nodes is equal to 50×50=2500 (h=2 nm) and time step is equal to 0.0005 ps.

In Figures 1 and 2 the heating curves at the point (2nm, 2nm) are shown. As can be seen, for the lowest laser intensity only the heating process is observed, while for the higher laser intensity the melting process appears (‘stop’ corresponding to the melting process). In the case of the largest laser intensity (Figure 2) the isothermal liquid-vapour phase change starts. Figures 3 and 4 illustrate the courses of electrons and lattice temperatures at the same point.

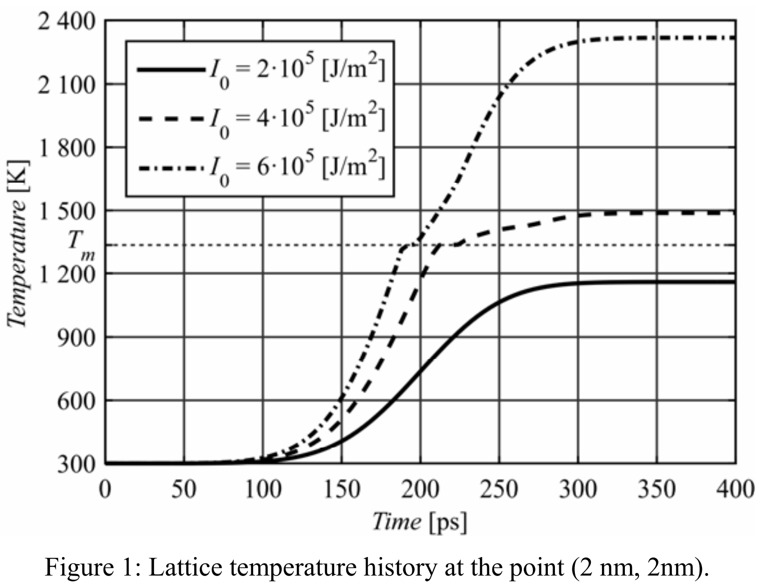

Figure 1: Lattice temperature history at the point (2 nm, 2nm).

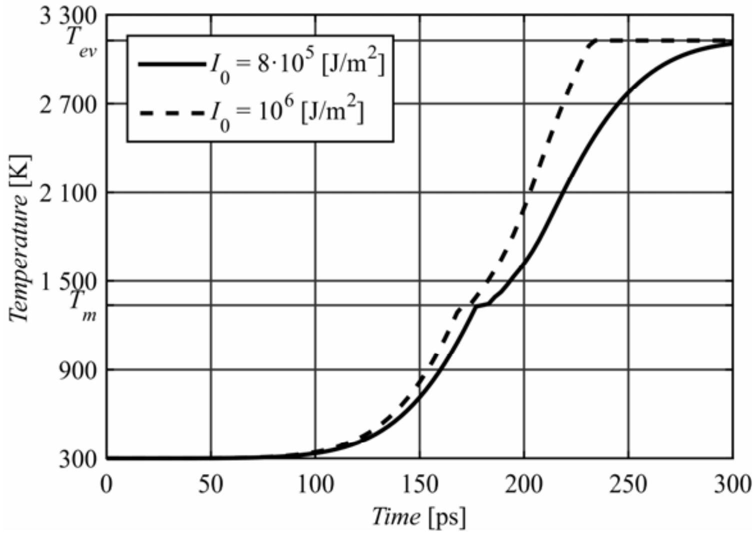

Figure 2: Lattice temperature history at the point (2 nm, 2nm).

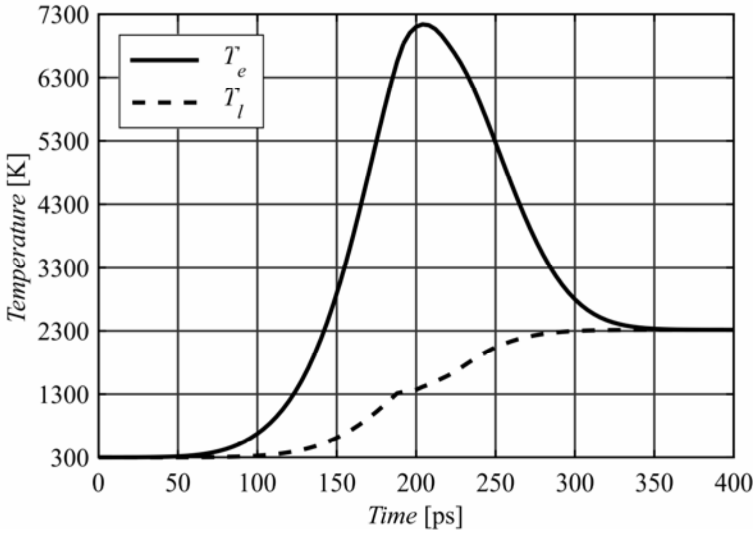

Figure 3: Temperature history at the point (2nm, 2nm) for $I_0 = 6\cdot10^5$ J/m^2.

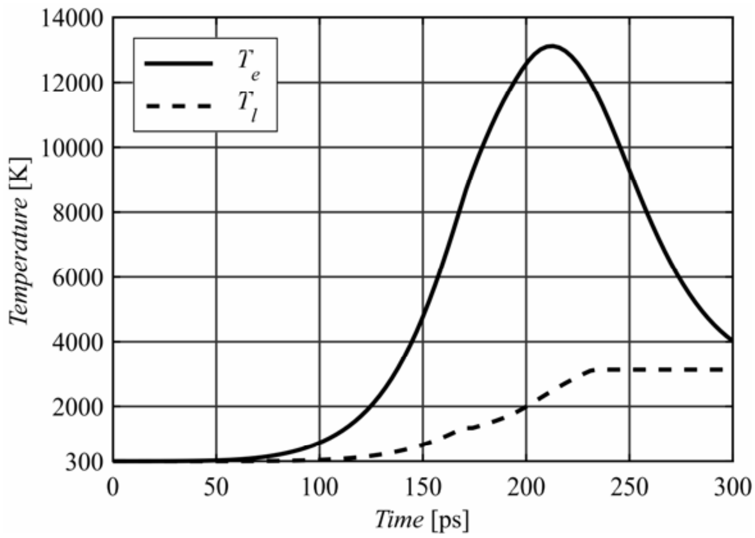

Figure 4: Temperature history at point (2nm, 2nm) for $I_0 = 10^6$ J/m^2.

In Figure 5 the electrons and phonons temperature distribution after 150 ps for laser intensity $I_0 = 8 \cdot 10^5$ J/m^2 is shown.

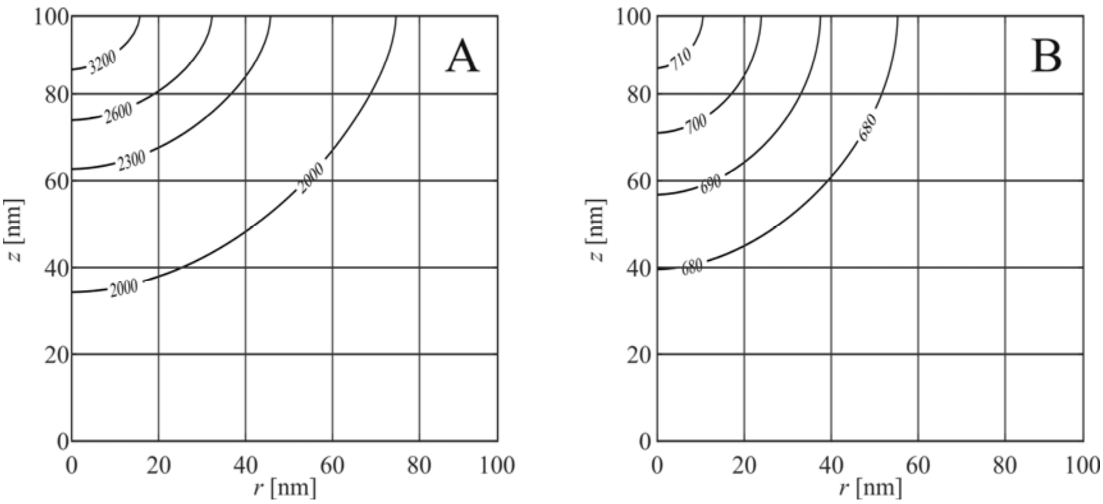

Figure 5: Temperature distribution after 150 ps, A) electrons, B) lattice.

6 FINAL REMARKS

The thermal processes occurring in the axisymmetric micro-domain subjected to the ultra-short laser pulse are analyzed. The problem is described by two equations for electrons and lattice temperatures supplemented by appropriate boundary and initial conditions. At the stage of numerical computations the finite difference method together with the procedures modeling the phase transitions is used.

In the future, the algorithm will be supplemented by a procedure modeling the ablation process.

ACKNOWLEDGEMENT

This work is supported by the project BK-255/RMT4/2016.

REFERENCES

[1] R.A. Escobar, S.S. Ghai, M.S. Jhon, C.H. Amon, Multi-length and time scale thermal transport using the lattice Boltzmann method with application to electronic cooling. *International Journal of Heat and Mass Transfer*, **49**, 97-107, 2006.

[2] G. Chen, D. Borca-Tasciuc, R.G. Yang, Nanoscale Heat Transfer. *Encyclopedia of NanoScience and Nanotechnology*, 17, 429–459, 2004.

[3] Z.M. Zhang, *Nano/microscale heat transfer, 1st Edition*. McGraw Hill, 2007.

[4] A.N. Smith, P.M. Norris, Microscale heat transfer. *A. Bejan, D. Kraus (Eds.), Heat Transfer Handbook, John Wiley & Sons, New Jersey*, **18**, 1309-1359, 2003.

[5] D.Y. Tzou, *Macro- to Microscale Heat Transfer: The lagging behavior, 2nd Edition*, Taylor and Francis, 1997.

[6] J.K. Chen, D.Y. Tzou, J.E. Beraun, A semiclassical two-temperature model for ultrafast laser heating. *International Journal of Heat and Mass Transfer*, **49**, 307-316, 2006.

[7] J.K Chen, W.P. Latham, J.E. Beraun, The role of electron–phonon coupling in ultrafast laser heating. *Journal of Laser Applications*, **17(1)**, 63-68, 2005.

[8] J. Huang, K. Baheti, J.K. Chen, Y. Zhang, An axisymmetric model for solid-liquid-vapor phase change in thin metal films induced by an ultrashort laser pulse. *Frontiers in Heat and Mass Transfer*, **2**, 013005, 2011.

[9] E. Majchrzak, J. Dziatkiewicz, Ł. Turchan, Sensitivity analysis and inverse problems in microscale heat transfer. *Defect and Diffusion Forum*, **362**, 209-223, 2015.

[10] J. Dziatkiewicz, W. Kuś. E. Majchrzak, T. Burczyński, Ł. Turchan, Bioinspired identification of parameters in microscale heat transfer. *International Journal for Multiscale Computational Engineering*, **12(1)**, 79-89, 2014.

[11] C.P. Grigoropoulos, A. Chimmalgi, D.J. Hwang, Nano-structuring using pulsed laser radiation. *Laser Ablation and its Applications, Springer Series in Optical Sciences*, **129**, 473-504, 2007.

[12] E. Majchrzak, B. Mochnacki, Modeling of melting and resolidification in domain of metal film subjected to a laser pulse. *Archives of Foundry Engineering*, **16(1)**, 41-44, 2016.

[13] A. Tarzia, A. Domingo, A Bibliography on Moving-Free Boundary Problems for the Heat-Diffusion Equation. The Stefan and Related Problems. *MAT, Series A: Conferencias, seminarios y trabajos de matemática*, **2**, 1–297, 2000.

[14] B. Mochnacki, R. Szopa, Generalized micro/macro model of crystallization and its numerical realization. *International Journal for Multiscale Computational Engineering*, **8(3)**, 259-266, 2010.

[15] B. Mochnacki, E. Majchrzak, Identification of macro and micro parameters in solidification model. *Bulletin of the Polish Academy of Sciences, Technical Sciences*, **55(1)**, 107-113, 2007.

[16] E. Majchrzak, J. Dziatkiewicz, Analysis of ultashort laser pulse interactions with metal films using a two-temperature model. *Journal of Applied Mathematics and Computational Mechanics*, **14(2)**, 31-39, 2015.

[17] E. Majchrzak, B. Mochnacki, J.S. Suchy, Computer simulation of heat transfer between the particles and metal matrix during the solidification of a cast composite. *International Journal of Cast Metals Research*, **12(4)**, 241-249, 1999.

[18] E. Majchrzak, Ł. Turchan, J. Dziatkiewicz, Modeling of skin tissue heating using the generalized dual-phase lag equation. *Archives of Mechanics*, **67(6)**, 417-437, 2015.

[19] B. Mochnacki, M. Ciesielski, Numerical model of thermal processes in domain of thin film subjected to a cyclic external heat flux. *THERMEC 2011, PTS 1-4 Book Series: Materials Science Forum*, **706–709**, 1460–1465, 2012.

[20] J.K. Chen, J.E. Beraun, Numerical study of ultrashort laser pulse interactions with metal films. *Numerical Heat Transfer, Part A*, **40**, 1-40, 2001.